JOURNAL OF Applied Polymer SCIENCE

# Related physicochemical, rheological, and dielectric properties of nanocomposites of superparamagnetic iron oxide nanoparticles with polyethyleneglycol

Taraneh Javanbakht,[1] Sophie Laurent,[2,3] Dimitri Stanicki,[2] Eric David[1]
[1]Department of Mechanical Engineering, École de Technologie Supérieure, Montréal, Quebec, Canada H3C 1K3
[2]Laboratory of NMR and Molecular Imaging, University of Mons, Avenue Maistriau 19, B-7000 Mons, Belgium
[3]Center for Microscopy and Molecular Imaging (CMMI), 6041 Gosselies, Belgium
Correspondence to: T. Javanbakht (E-mail: taraneh.javanbakht@etsmtl.ca)

**ABSTRACT:** In this study, we present the physicochemical, rheological, and dielectric properties of the superparamagnetic iron oxide nanoparticles (SPIONs) coated with polyethyleneglycol (PEG). It was observed that the increase of the concentration of PEG prohibited the sedimentation of nanoparticles, which increased the colloidal stability of nanocomposites. The surface study of the polymer and the nanocomposites using TOF-SIMS showed that the samples did not have the same surface properties. The analysis of the intensity ratios of the $FeO^+/Fe^+$ and $OH^-/O^-$ peaks of the nanocomposites of bare, positively, and negatively charged SPIONs with PEG revealed that no reduction occurred for these nanoparticles when coated with PEG, whereas the iron atoms on the surface of PEG negatively charged SPIONs were less oxidized than those on the surface of PEG-bare SPIONs, and the iron atoms on the surface of PEG positively charged SPIONs were more oxidized than the second ones. The rheological study of the polymer and the nanocomposites revealed that the presence of SPIONs did not change the rheological behavior of PEG. The analysis of the dielectric properties of PEG and its composites with SPIONs showed that when SPIONs particles (bare and positively charged) were included in PEG, low frequency dispersion (LFD) was strongly enhanced, that the iron oxide nanoparticles reduced the impedance of PEG in the nanocomposites and that the difference in their surface charge affected their impedance. Taken together, these results suggest that the nanocomposites of PEG with SPIONs have appropriate properties for fluid modification and applications in the nanotechnology and photovoltaic devices. © 2019 Wiley Periodicals, Inc. J. Appl. Polym. Sci. **2019**, *136*, 48280.

**KEYWORDS:** composites; microscopy; spectroscopy; thermoplastics

Received 30 January 2019; accepted 30 June 2019
**DOI: 10.1002/app.48280**

## INTRODUCTION

The development of nanocomposites that possess significantly improved properties due to dispersed nanoparticles has attracted significant interest over the last decades. Nanocomposites consist of a polymeric matrix and an inorganic filler of typical size 1–100 nm. They have better mechanical properties than conventional composites (microcomposites or macrocomposites).[1] The large surface to volume ratio of nanoparticles that are used in the preparation of nanocomposites plays an important role for their surface reactivity. Several parameters in the formation of polymer nanocomposites such as the effects of nanofiller on chain dynamics and the dependence of their final properties on their degree of dispersion were also determined previously.[2]

Hydrogels are polymers that can swell in water, retain a significant fraction of water in their structure, but not dissolve in it.[3] The superabsorbent property of hydrogels renders them useful in conserving water as well as solving other environmental issues. Chemically and physically crosslinked hydrogels are two kinds of these molecules that have been widely used to create stable environmental systems for biomolecules delivery. The junctions in physically crosslinked hydrogels consist of ionic interactions, hydrophobic association, or coiled-coil interactions.[4–6] Polyethyleneglycol (PEG) is a polar organic biocompatible polymer widely used for the preparation of nanocomposites.[7,8]

The approach for the preparation of the nanocomposites of superparamagnetic iron oxide nanoparticles (SPIONs) with PEG includes refluxing at high temperature,[9] coating with oleic acid, and recoating with PEG.[10] The SPION coating includes *in situ* coating, postsynthesis adsorption, and postsynthesis end grafting.[11] The incorporation of SPIONs to PEG can be carried out via either the encapsulation of

nanoparticles within the hydrogel or their infiltration into it during swelling.[12] Gonzalez-Tello *et al.* demonstrated previously the pseudo-Newtonian rheological behavior of PEG.[13] The rheological behavior of the nanocomposites of SPIONs with PEG has not been studied, yet. Moreover, these properties have not been related to the physicochemical properties of these nanocomposites.

During the recent years, the biomedical applications of the nanocomposites of PEG with SPIONs have been investigated. It has been shown that using PEG increases the biocompatibility of SPIONs for these applications.[14,15] It has been also confirmed that by controlling the apparent viscosity of the viscous materials, such as hydrogels, the rates of endocytosis, including nonspecific pinocytosis and specific receptor-mediated endocytosis, are increased. Moreover, increasing the viscosity of biomolecules provides a physical barrier limiting their diffusion into cells.[16,17] Therefore, the related physicochemical, rheological, and dielectric properties of the SPIONs nanocomposites, previously studied for drug delivery into cells, were important to be investigated.

In this article, the nanocomposites of PEG with bare, positively, and negatively charged SPIONs have been prepared, and their colloidal stability has been determined. To our knowledge, this is the first time that the related physicochemical, rheological, and dielectric properties of PEG and its nanocomposites with SPIONs are investigated. The relation between the surface charge and morphology of SPIONs with the formation of colloidal solutions was investigated. The role of these nanoparticles on the rheological properties of nanocomposites with PEG was also studied.

## EXPERIMENTAL

### Materials

PEG was purchased from Fisher Scientific (Fair Lawn, United States). For the synthesis of SPIONs, these chemicals were used: methanol HPLC purchased from ChemLab (Dijon, France), acetone (ACS reagent, ≥99.0%), diethylic ether (ACS reagent, ≥99.0%), dimethylformamide anhydrousHPLC, n-[3-(trimethoxysilyl)propyl] ethylenediamine (TPED) (97%), all purchased from Sigma-Aldrich (Overijse, Belgium), diethylene glycol (>99%), iron (II) chloride tetrahydrated (99%), both purchased from Merck (Overijse, Belgium), solution of iron (III) chloride (45%) purchased from Riedel-de Haën (Leuven, Belgium), 1-ethyl-3-(3-dimethylaminopropyl) carbodiimide (>98%), tetramethylammonium hydroxide (>95%) purchased from TCI Chemicals (Zwijndrecht, Belgium), 3-(triethoxysilyl)propyl succinic anhydride (TEPSA) (>94%) purchased from ABCR (Karlsruhe, Germany).

### Nanoparticle Preparation

Bare SPIONs: 5 mL of an aqueous solution of $FeCl_2.4H_2O$ (0.045 M) and $FeCl_3.6H_2O$ (0.0375 M) were added to 250 mL of diethyleneglycol. The mixture was heated to 170 °C and maintained at this temperature for 15 min before the addition of the base (i.e., solid NaOH until a final concentration of 0.375 M). Subsequently, temperature was maintained at 170 °C for a period of 1 h before cooling to 60 °C. The synthesized SPIONs were collected with a neodymium magnet and washed with 100 mL of a $HNO_3$ (1 M) solution.

Negatively charged SPIONs (with carboxylate functions)[18]: 14.2 mL of 3-(triethoxysilyl)propylsuccinic anhydride (TEPSA, 50 mmol) were slowly added to a nanoparticle suspension in DMF (100 mM of iron in 100 mL). A total of 8.6 mL of water followed by 5 mL of TMAOH solution (1 M) were added at room temperature and under homogenization. The solution was heated to 100 °C for 24 h under continuous stirring. The SPIONs were precipitated by the addition of acetone/ether (50/50) mixture and collected with a neodymium magnet. The precipitate was washed with acetone several times and finally dispersed in water. Excess of silane derivative and other chemicals were removed by membrane filtration (cut-off of the membrane is 30 000 Da).

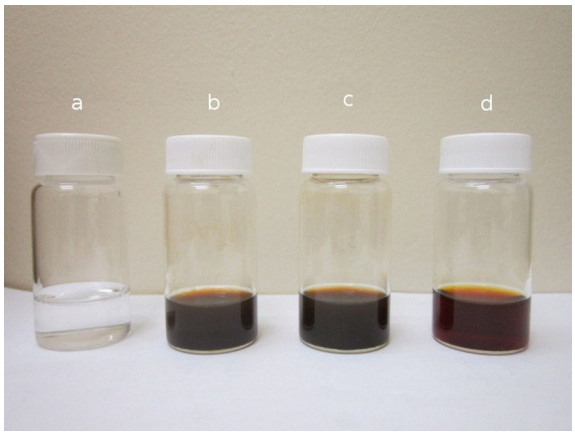


**Figure 1.** (a) PEG, nanocomposites of (b) PEG-bare SPIONs, (c) PEG-positively charged SPIONs and (d) PEG-negatively charged SPIONs. [Color figure can be viewed at wileyonlinelibrary.com]

Positively charged SPIONs (with amino functions): N-[3-(trimethoxysilyl)propyl] ethylenediamine (TPED) was grafted onto SPIONs by adding 25 mmol of TPED (5.4 mL) to a suspension of NP (100 mL, [Fe] = 25 mM) at 50 °C. After stirring for 2 h at reflux, the mixture was cooled at room temperature, and the suspension was purified by membrane filtration (membrane cut-off: 30 kDa), and then centrifuged (16 500 g; 45 min).[19]

**Nanocomposite Preparation.** A total of 4.8 g of PEG was mixed with 20 mL of deionized water (18.2 MΩ $cm^{-1}$) during 15 min at room temperature. The polymer solution was divided into four portions: one portion without SPIONs and three portions for the preparation of the nanocomposites. Each portion of the polymer

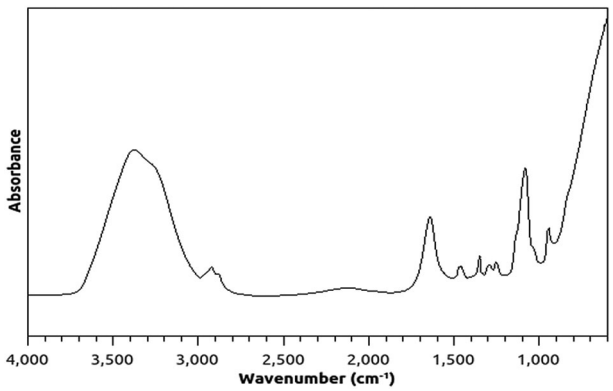


**Figure 2.** FTIR spectrum of the nanocomposites of PEG with bare SPIONs.

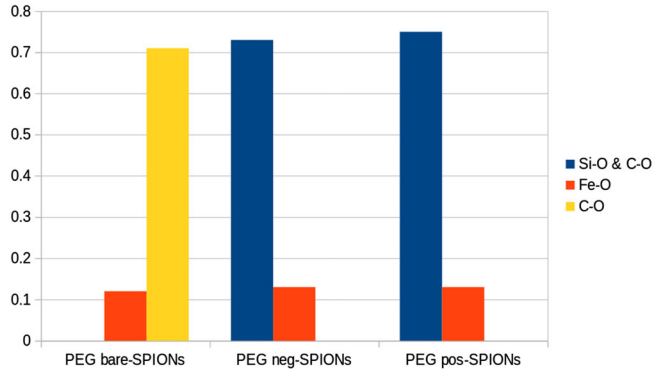


**Figure 3.** The normalized intensity ratios of the Si-O & C-O, Fe-O and C-O peaks of the nanocomposites of PEG with SPIONs. [Color figure can be viewed at wileyonlinelibrary.com]

solution contained 1.2 g of the polymer dissolved in 5 mL of water. A total of 12 mg of bare, positively charged or negatively charged SPIONs were added separately to each of the three portions of PEG solution to obtain the nanocomposite solutions (1% w/w). Then, they were mixed during 15 min at room temperature. The forth PEG solution was kept for the analysis of the polymer. The increase of the concentration of PEG from 0.1 to 1% prohibited the sedimentation of nanoparticles and increased the colloidal stability of nanocomposites.

### Dispersion of Nanocomposites

The dispersion of nanocomposites in water was studied after their preparation in water. The stability of the samples was determined according to their dispersion in this solvent.

### Fourier Transform Infrared (FTIR) Spectroscopy

Using a Perkin Elmer spectrum 65 FTIR spectrometer, attenuated total absorbance probe, in the range of 600–4000 $cm^{-1}$ FTIR spectroscopy was carried out at 4 $cm^{-1}$ resolution were recorded. Thirty two scans were co-added to improve S/N.[19–21]

### Scanning Electron Microscope Imaging

A JEOL JSM-7600TFE SEM was used to obtain photomicrographs. Samples were deposited onto an aluminum substrate and inserted into the instrument. Images were obtained at 2 and 5 kV accelerating voltages.[19]

### Time-of-Flight Secondary Ion Mass Spectrometry (TOF-SIMS)

Positive and negative ion spectra were obtained on an ION-TOF IV TOF-SIMS using a 15 kV $Bi^+$ primary ion source, so as to acquire masses up to 100, while maintaining the primary ion dose at less than $10^{12}$ ions/$cm^2$ in order to ensure static conditions. All the positive ion spectra were calibrated to the $H^+$, $C^+$, $CH^+$, $CH_2^+$, $CH_3^+$, $C_2H_5^+$, and $C_3H_5^+$ peaks, and all the negative ion spectra were calibrated to the $C^-$, $C_2^-$, $CH^-$, $C_2H^-$, $C_3^-$, and $C_3H^-$ peaks before data analysis. Sample spectra were taken over an area 50 μm × 50 μm, with an emission current of 1.0 μA in bunch mode, rastered in random mode, and presented as 128 by 128 pixels.[19]

### Rheology of Nanocomposites

A MCR-502 rheometer was used for the circular rheological measurements of PEG and nanocomposites of SPIONs with PEG at 20 °C. The measurements were carried out with 4 μL of each sample in triplicata using a rough pistone. The QtiPlot software was used to determine the standard deviation of data.

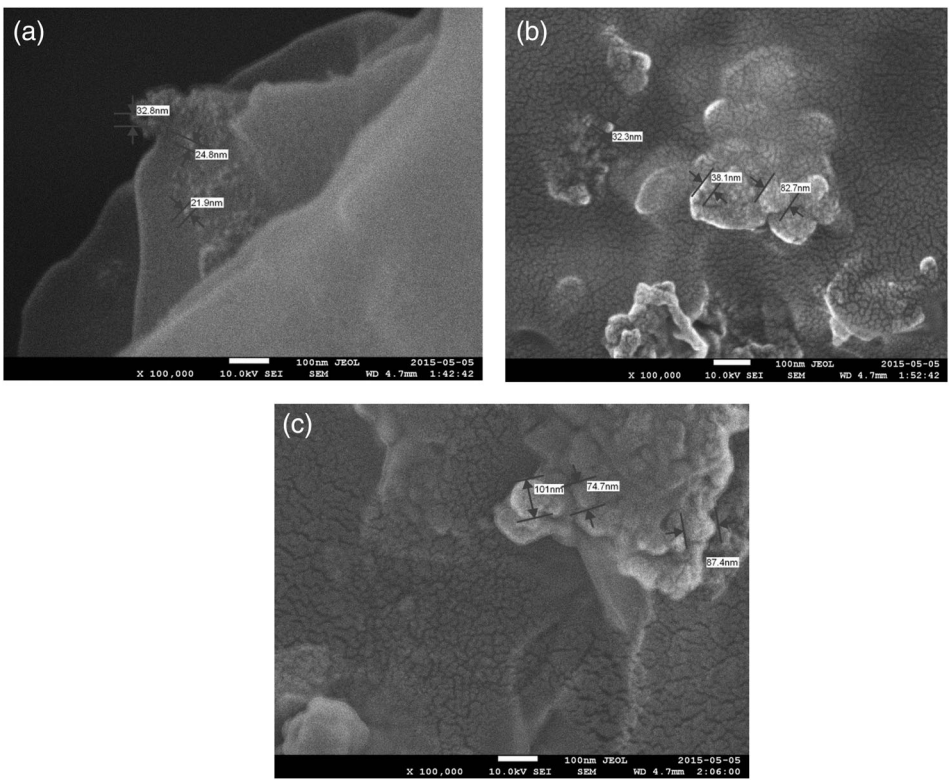


**Figure 4.** SEM images of the nanocomposites of (a) bare, (b) positively, and (c) negatively charged SPIONs with PEG.

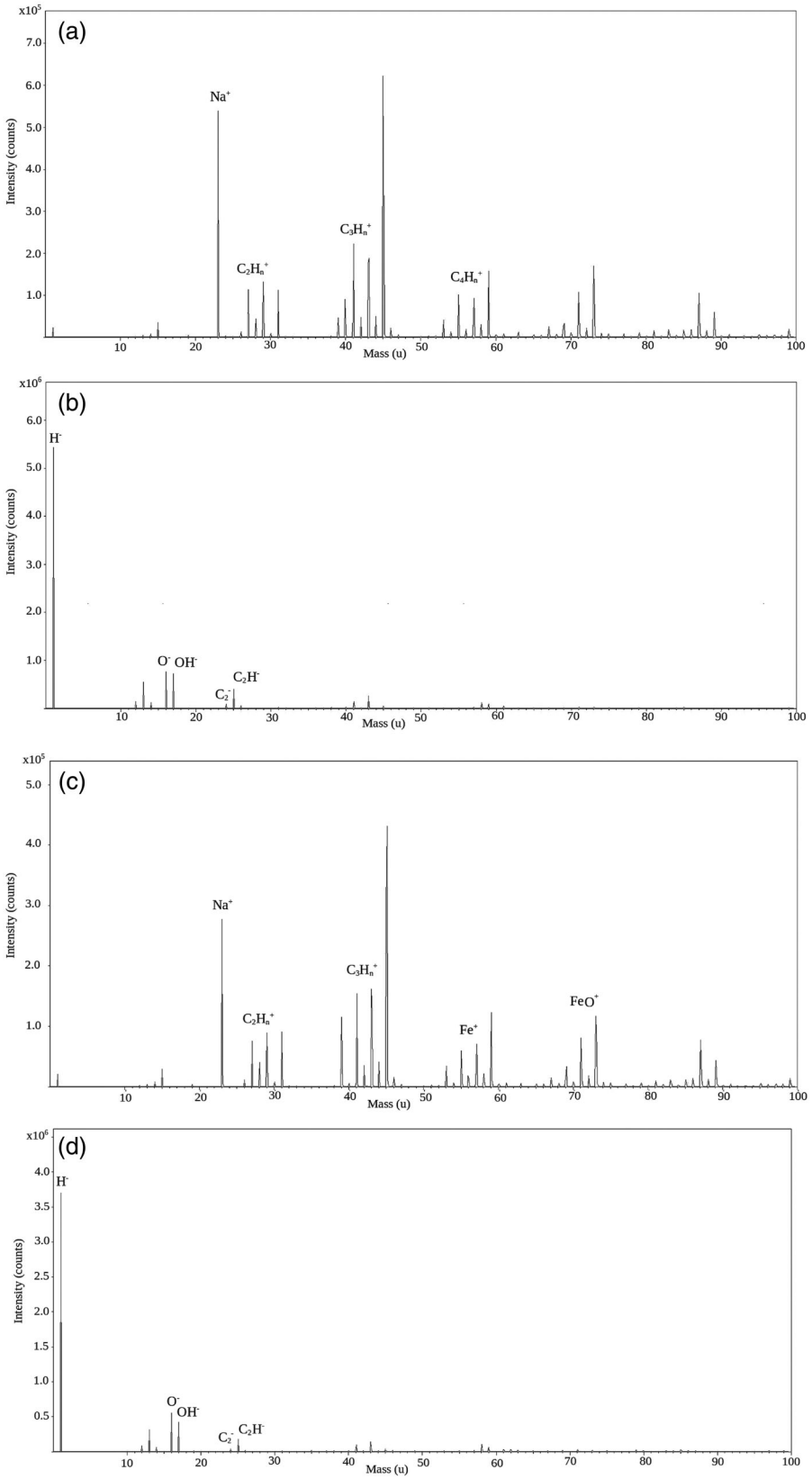


**Figure 5.** Positive and negative TOF-SIMS spectra of (a, b) PEG, the nanocomposites of (c, d) bare, (e, f) positively, and (g, h) negatively charged SPIONs with PEG.

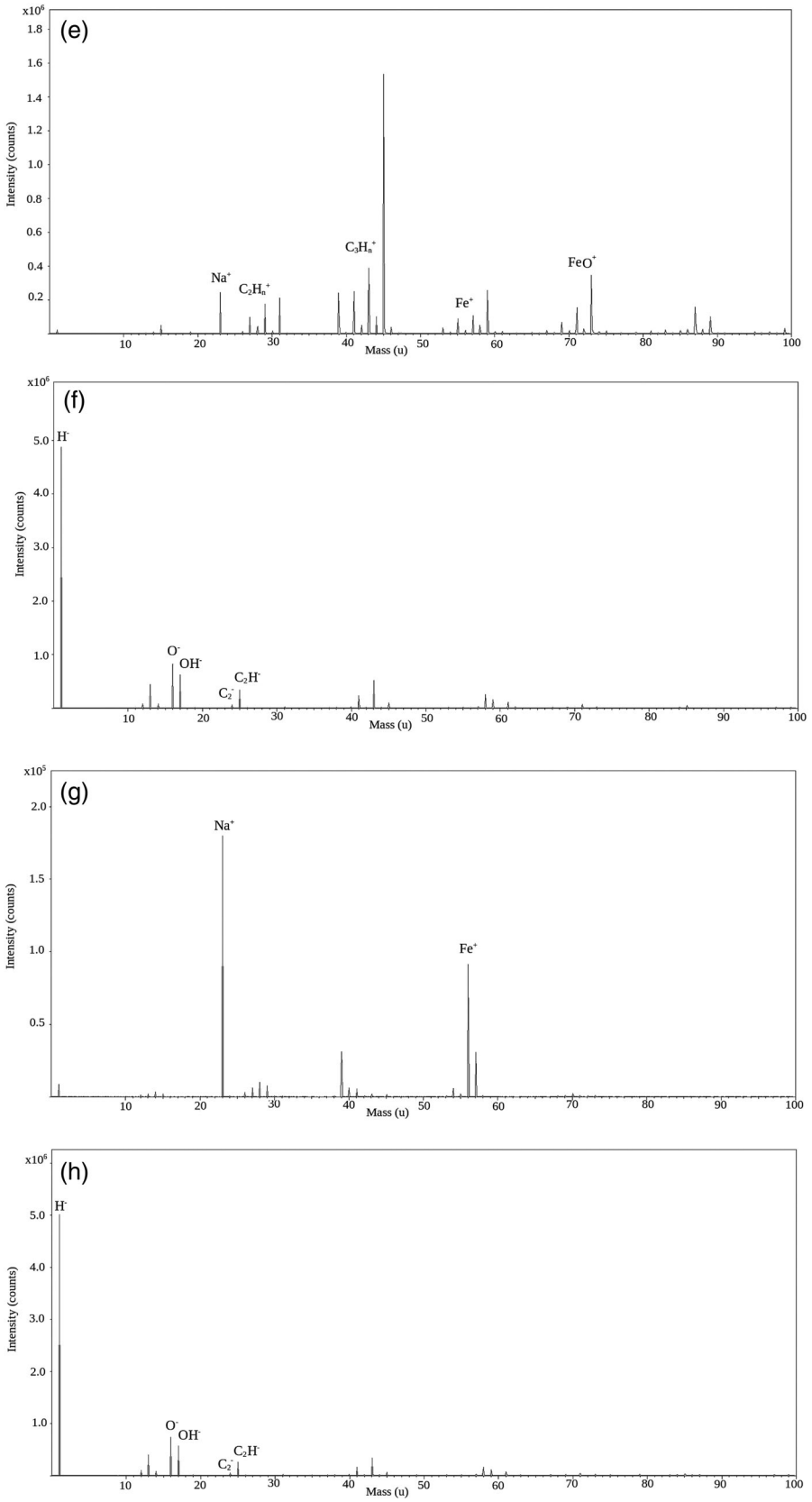


**Figure 5.** (Continued)

**Table I.** The Intensities of the $FeO^+$, $Fe^+$, $OH^-$, and $O^-$ Peaks of Nanocomposites of Bare, Positively, and Negatively Charged SPIONs With PEG

| Sample | $FeO^+$ | $Fe^+$ | $OH^-$ | $O^-$ |
|---|---|---|---|---|
| PEG | — | — | $6.7 \times 10^5$ | $7.5 \times 10^5$ |
| PEG bare SPIONs | $1.3 \times 10^4$ | $1.3 \times 10^4$ | $4.4 \times 10^5$ | $5.6 \times 10^5$ |
| PEG negatively charged SPIONs | $2.7 \times 10^2$ | $9.2 \times 10^4$ | $6.2 \times 10^5$ | $7.7 \times 10^5$ |
| PEG positively charged SPIONs | $1.3 \times 10^4$ | $7.5 \times 10^3$ | $6.2 \times 10^5$ | $8.5 \times 10^5$ |

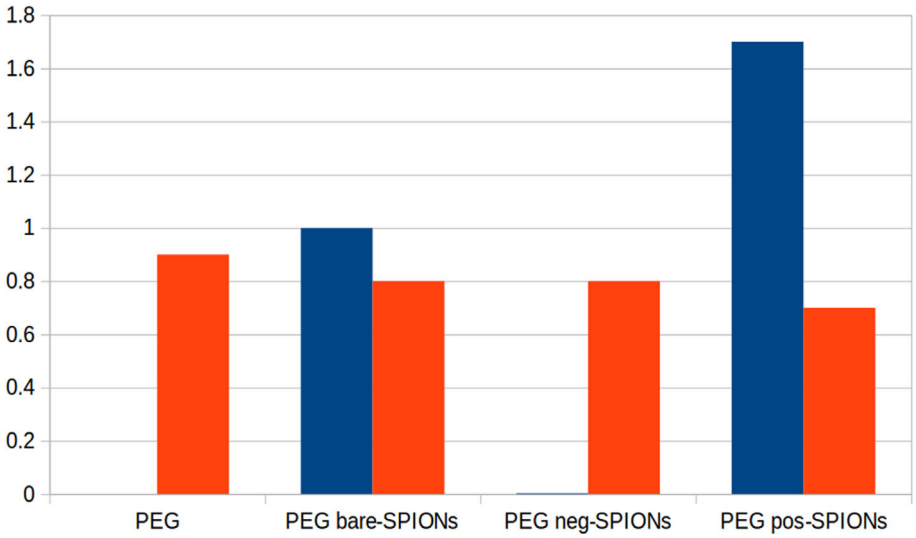


**Figure 6.** The intensity ratio change of the (a) $FeO^+/Fe^+$ and (b) $OH^-/O^-$ peaks of nanocomposites of bare, positively, and negatively charged SPIONs with PEG. [Color figure can be viewed at wileyonlinelibrary.com]

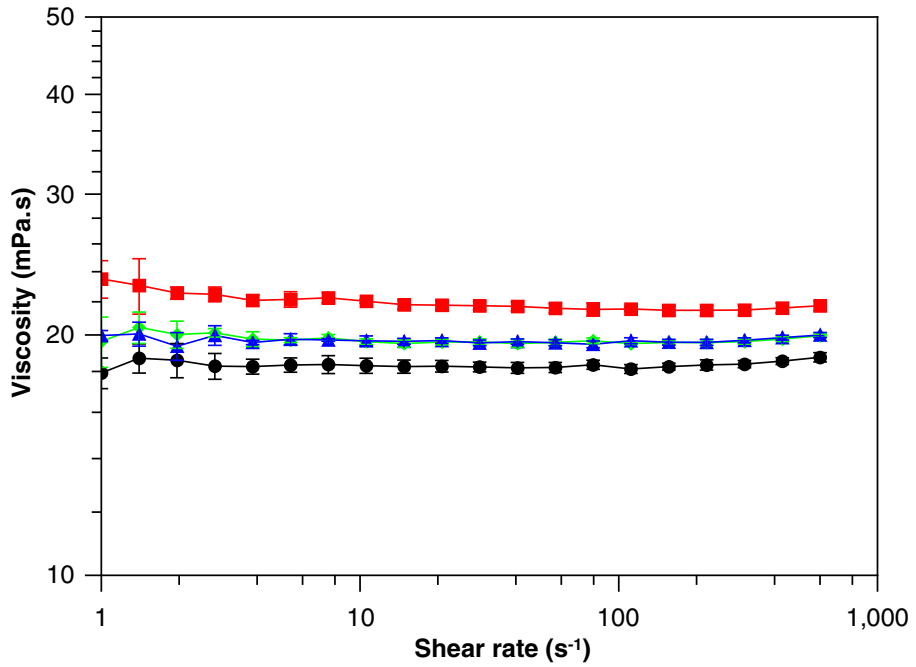


**Figure 7.** Viscosity versus shear rate of PEG and its nanocomposites. The black, red, green, and blue lines represent the data for PEG and nanocomposites of bare, positively, and negatively charged SPIONs with PEG, respectively. [Color figure can be viewed at wileyonlinelibrary.com]

### Dielectric Properties Measurements

The broadband dielectric spectroscopy (BDS) was carried out using a Novocontrol converter and Alpha-N High Dielectric Analyzer. The samples were deposited on circular aluminum electrodes measuring 30 mm in diameter. The average of the measured data over 5 points were registered in the range from 0.01 Hz to $3 \times 10^5$ Hz.[22]

## RESULTS AND DISCUSSION

### Nanocomposite Preparation

The stability of the nanocomposites concerning their dispersion in water was not the same. The nanocomposites of bare and positively charged SPIONs were stable during 6 h as they were dispersed in water but after 6 h, they were sedimented, whereas those of negatively charged SPIONs were permanently stable and dispersed in this solvent. The difference in the dispersion of nanocomposites was attributed to their surface charge and electrostatic interactions. Figure 1 shows the images of samples: (a) PEG, nanocomposites of (b) PEG-bare SPIONs, (c) PEG-positively charged SPIONs and (d) PEG-negatively charged SPIONs, respectively.

### FTIR Analysis of the SPIONS

Figure 2 shows the FTIR spectrum of the nanocomposites of PEG with the bare SPIONs. The FTIR spectrum of PEG as well as those of this polymer with the positively and negatively charged SPIONs represents the same peaks. The peaks at around 1330 and 1100 $cm^{-1}$ in the spectrum of PEG are attributed to C—H bending and C—O stretching vibration, respectively. The peaks at 2888 and 2910 $cm^{-1}$ are attributed to the alkyl chain of polymer.[23] Both Si—O and C—O peaks appeared in the same region for the nanocomposites of PEG with the positively and negatively charged SPIONs. The Si—O peak was absent in the spectrum of the nanocomposite of PEG with the bare SPIONs (results not shown). The peaks at 1050 and 1330 $cm^{-1}$ are attributed to the Fe—O and the C—O bonds of the $CH_2$—OH groups, respectively. The Si—O vibrational bond, which is due to the silica shell on the surface of positively and negatively charged SPIONs, appears at around 1100 $cm^{-1}$.[19] The absorption around 1474 $cm^{-1}$ is due to binding vibration of —$CH_2$, and the broad band at 3400–3500 $cm^{-1}$ corresponds to the presence of hydroxyl bonds, respectively.[20,24]

Figure 3 represents the normalized intensity ratios of the Si—O and C—O, Fe—O and C—O peaks of the nanocomposites of PEG with SPIONs. The intensity ratio of the superposed Si—O & C—O peaks of the nanocomposite of the positively charged SPIONs with PEG was higher than that of the nanocomposite of the negatively charged SPIONs with PEG and that of the second ones was higher than that of the C—O peak of the nanocomposite of the bare SPIONs with PEG. The intensity ratios of the Fe—O peaks of the positively and negatively charged SPIONs with PEG were a bit higher than that of the nanocomposite of the bare SPIONs with the polymer. This indicates that the amount of the iron oxide nanoparticles in the nanocomposite of the positively charged SPIONs with PEG could be a bit more than those in the other nanocomposites.

### SEM Imaging

Figure 4 shows the SEM images of the nanocomposites of (a) bare, (b) positively, and (c) negatively charged SPIONs with PEG. The sizes of nanocomposites were more than those of nanoparticles alone, which was around 15 nm (data not shown). This shows that the coating of SPIONs with PEG was carried out successfully.

### TOF-SIMS Analysis of Nanocomposites

Figure 5 shows the positive and negative TOF-SIMS spectra of of (a,b) PEG, and the nanocomposites of (c,d) bare, (e,f) positively, and (g,h) negatively charged SPIONs with PEG. The peaks of hydrocarbons ($C_nH_n^+$) and $Na^+$ (m/e 23) were observed in the positive spectra [Figure 5(a-g)] and those of $H^-$ (m/e 1), C- (m/e 16), $O^-$ (m/e 16), $OH^-$ (m/e 17), $H^-$ (m/e 1), $C^-$ (m/e 12), $CH^-$ (m/e 13), $O^-$ (m/e 16), $OH^-$ (m/e 17), $C_2^-$ (m/e 24), and $C_2H^-$ (m/e 25) in the negative spectra [Figure 5(b,d,f,h)], respectively. In positive spectra of nanocomposites of bare and positively charged SPIONs with PEG, the peaks of $Si^+$ (m/e 28), $SiO^+$ (m/e 44), $Fe^+$ (m/e 56), $FeO^+$ (m/e 72), and $FeOH^+$ (m/e 73) were also observed. The peaks of $Si^+$ (m/e 28) and $Fe^+$ (m/e 56) were also observed in the positive spectrum of nanocomposites of negatively charged SPIONs with PEG [Figure 5(c,e)]. The other peaks were observed in the logarithmic mode of this spectrum [Figure 5(g)].

The pattern of hydrocarbons was present on the TOF-SIMS positive spectra of samples. This is due to the high surface reactivity of SPIONs that caused the adsorption of hydrocarbons on the surface of these nanoparticles. The peak of $NH_2^+$ (m/e 16) disappeared in the spectrum of the nanocomposite of the positively charged SPIONs with PEG [Figure 5(e)], whereas the peak of $COOH^-$ (m/e 45) was still present in the spectrum of the negatively charged SPIONs with this polymer [Figure 5(h)]. Moreover, the intensity of the peak $Fe^+$ (m/e 56) was more in the spectrum of the second nanocomposites [Figure 5(g)] than in the spectrum of the first ones [Figure 5(e)]. This showed that PEG affected the positively charged SPIONs more than the negatively charged ones.

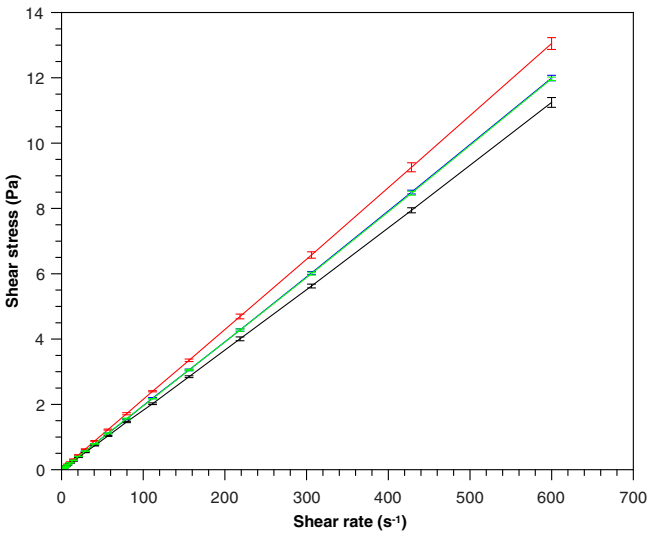


**Figure 8.** Shear stress versus shear rate of PEG and nanocomposites of PEG with bare, positively, and negatively charged SPIONs. The black, red, green, and blue lines represent the data for PEG and nanocomposites of bare, positively, and negatively charged SPIONs with PEG, respectively. [Color figure can be viewed at wileyonlinelibrary.com]

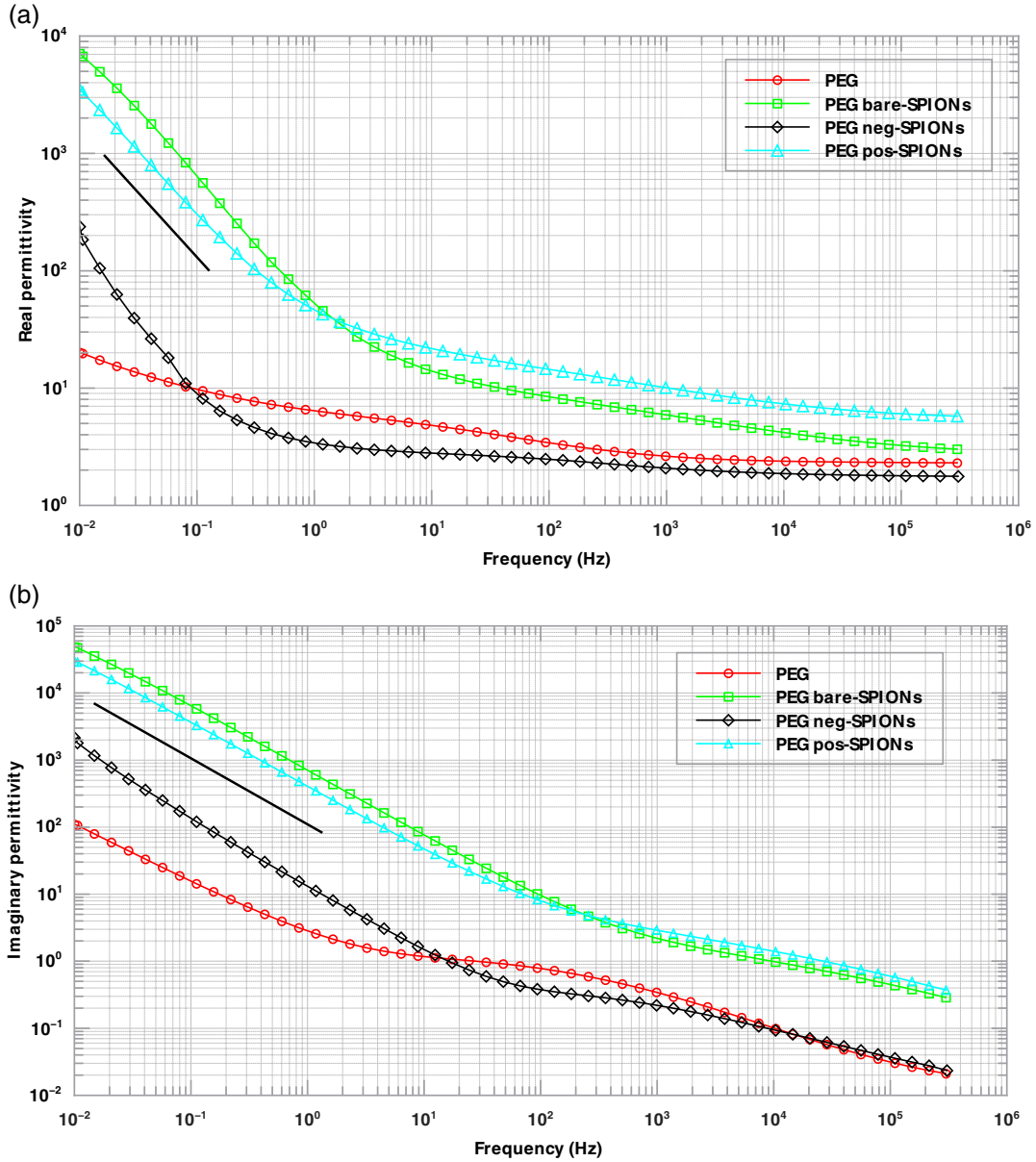


**Figure 9.** The BDS spectra of PEG and its composites: (a) real part of the relative permittivity, (b) imaginary part of the relative permittivity. [Color figure can be viewed at wileyonlinelibrary.com]

Table I represents the intensities of the $FeO^+$, $Fe^+$, $OH^-$, and $O^-$ peaks of nanocomposites of bare, positively, and negatively charged SPIONs with PEG.

Figure 6 shows the intensity ratio change of the $FeO^+/Fe^+$ and $OH^-/O^-$ peaks of nanocomposites of bare, positively, and negatively charged SPIONs with PEG. The intensity ratios of the $OH^-/O^-$ peaks of PEG bare SPIONs and PEG negatively charged SPIONs were the same, whereas that of PEG positively charged SPIONs was a bit lower than the first and second ones. This indicates that no reduction occurred for these nanoparticles when coated with PEG. The intensity ratio of the $FeO^+/Fe^+$ peaks of PEG negatively charged SPIONs was much less than that of PEG bare SPIONs, whereas that of PEG positively charged SPIONs was more than the second ones. This indicates that the iron atoms on the surface of PEG negatively charged SPIONs were less oxidized than those on the surface of PEG bare SPIONs and that the iron atoms on the surface of PEG positively charged SPIONs were more oxidized than the second ones.

### Rheological Analysis of Nanocomposites

Figure 7 shows the diagram of viscosity of PEG and nanocomposites of PEG with bare, positively, and negatively charged SPIONs versus shear rate. The pseudo-Newtonian behavior at 20 °C was observed for all the samples. This result revealed that the shear rate has no effect on the viscosity values of these nanocomposites or the polymer alone. As observed in Figure 7, the presence of SPIONs did not change the rheological behavior of PEG, which resulted in the similarity of the

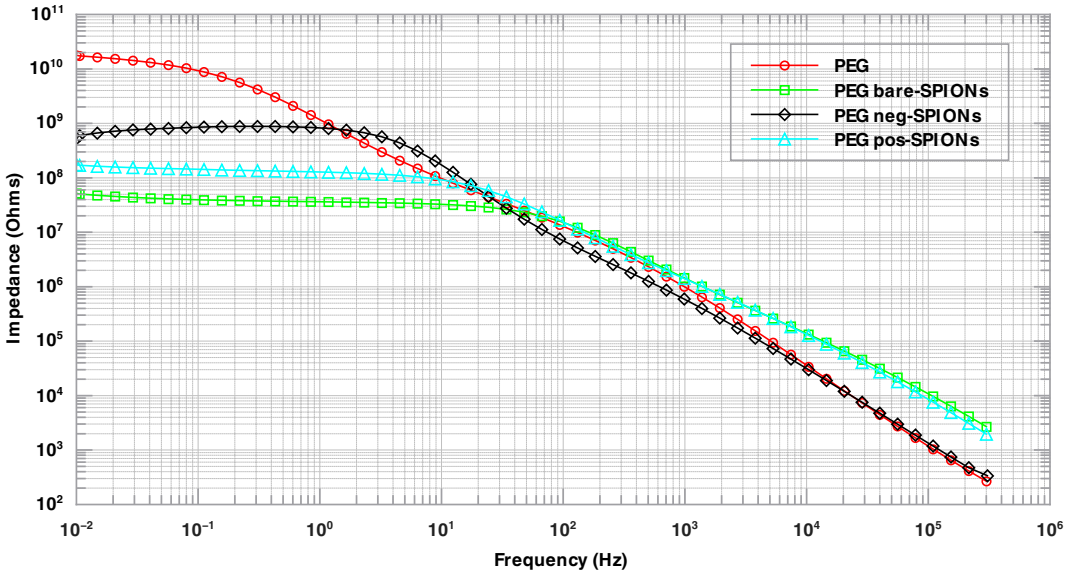


**Figure 10.** Impedance versus frequency of PEG and its composites with bare, positively, and negatively charged SPIONs. [Color figure can be viewed at wileyonlinelibrary.com]

rheological behavior of nanocomposites of SPIONs with PEG in comparison with that of the polymer. As expected, the viscosity values of PEG were somehow less than those of the nanocomposites.

Figure 8 shows the variation of the shear stress versus the shear rate of PEG and nanocomposites of PEG with bare, positively, and negatively charged SPIONs. The shear flow curves and the rheological parameters are average values of the experiments. As reported in Figure 8, the different shear flow curves were superimposed within the shear stress range investigated, indicating that the nanocomposites were stable during the experimental work. Shear stress increased constantly with shear rate up to 600 $s^{-1}$. This behavior was attributed to a dynamically stable region and may be related to a homogeneous field of velocities during the viscometric flow of yielding materials. The continuous increase of shear stress in the steady condition and the appearance of stability explains the similar behavior of PEG and its nanocomposites with SPIONs.

### Dielectric Properties Measurements

Figure 9 represents the BDS spectra at 23 °C of PEG and its composites with bare, positively, and negatively charged SPIONs. The black lines indicate the − 1 slope in log–log plots. For the neat polymer, the α relaxation process can be observed in the vicinity of 100 Hz as well as low frequency dispersion (LFD) at lower frequencies. A complete set of data on the dielectric response of PEG, including 3D plots, can be found elsewhere.[25] When SPIONs particles with a high positive zeta potential (bare and positively charged)[19] were included in PEG, their LFD was strongly enhanced. This dielectric behavior is characterized by a simultaneous increase of the real and the imaginary part of the relative permittivity exhibiting Kramer-Kronig consistency in complete contrast with direct conductivity. However, negatively charged SPIONs included in PEG were found to have little effect on the material dielectric response.

Figure 10 shows the variation of the impedance of PEG and its composites with bare, positively, and negatively charged SPIONs versus frequency. The impedance values of all samples were constant at low frequencies and decreased at high frequencies. At low frequencies, PEG showed higher impedance than the nanoparticles of SPIONs with PEG. This was expected as the iron oxide nanoparticles reduced the impedance of PEG in the nanocomposites. Moreover, the impedance of PEG negatively charged SPIONs was more than that of PEG positively charged SPIONs and that of the second ones were more than that of PEG-bare SPIONS. This indicates that the surface charge of SPIONs has impact on the impedance of their nanocomposites with the polymer.

A complete discussion on the physical origin of LFD can be found in a classic textbook on the dielectric behavior of solid matter.[26] In this particular case, it is related to ionic charge fluctuations that are strongly enhanced by positively charged nanoparticles. Electrode polarization could also be involved in the dielectric response, which would eventually lead to a relaxation peak at a lower frequency than $10^{-2}$ Hz.

## CONCLUSIONS

The present study involves the physicochemical, rheological, and dielectric properties of PEG, and its nanocomposites with bare, positively, and negatively charged SPIONs. The stability of samples concerning their dispersion in water was not the same. The nanocomposites of bare and positively charged SPIONs were stable during 6 h, whereas those of negatively charged SPIONs were permanently stable. The morphology and surface properties of samples determined the similarity of their physicochemical properties when coated with the polymer. As expected, the nanocomposites of SPIONs included in PEG did not have the same surface properties. Their surface properties were also different from those of PEG. Therefore, the peak intensities were different in the TOF-SIMS spectra of nanocomposites and PEG. The

rheological technique revealed the similarity of the viscosity values of nanocomposites with those of PEG alone, which confirmed that the presence of nanoparticles did not change the rheological behavior of the polymer. The continuous increase of shear stress in the steady condition and the appearance of stability were due to the similar behavior of PEG and its nanocomposites with SPIONs. When SPIONs particles with a high positive zeta potential (bare and positively charged) were included in PEG, their LFD was strongly enhanced. These nanocomposites with desired physico-chemical, rheological, and dielectric properties can have various applications such as fluid modification and applications in the nanotechnology and photovoltaic devices.

## ACKNOWLEDGMENTS

We acknowledge the $CM^2$ laboratory from the Ecole Polytechnique of Montreal for the SEM imaging of the samples. The authors thank the Center for Microscopy and Molecular Imaging (CMMI, supported by the European Regional Development Fund and the Walloon Region). This work was supported by the Fond National de la Recherche Scientifique (FNRS), UIAP VII, ARC Programs of the French Community of Belgium, COST actions (TD1402 and CA15209) and the Walloon region (Gadolymph and Holocancer programs).

## REFERENCES

1. Bokobza, L. *J. Appl. Polym. Sci.* **2004**, *205*, 61.
2. Fragiadakis, D.; Pissis, P.; Bokobza, L. *Polymer*. **2005**, *46*, 6001.
3. Nam, K.; Watanabe, J.; Ishihara, K. *Int. J. Pharm.* **2004**, *275*, 259.
4. Watanabe, T.; Ohtsuka, A.; Murase, N.; Barth, P.; Gersonde, K. *Magn. Reson. Med.* **1996**, *35*, 697.
5. Qu, X.; Wirsen, A.; Albertson, A.-C. *J. Appl. Polym. Sci.* **1999**, *74*, 3186.
6. Wang, C.; Steward, R. J.; Kopecek, J. *Nature*. **1999**, *397*, 417.
7. Bjugstad, K. B.; Redmond, D. E. Jr.; Lampe, K. J.; Kern, D. S.; Sladek, J. R. Jr.; Mahoney, M. *J. Cell Transpl.* **2008**, *17*, 409, 415.
8. Chan, R. T. H.; Marçal, H.; Russell, R. A.; Holden, P. J.; Foster, L. *J. R. Intern. J. Polym. Sci.* **2011**, *2011*, 1.
9. Park, J. Y.; Daksha, P.; Lee, G. H.; Woo, S.; Chang, Y. *Nanotechnology*. **2008**, *19*, 365603.
10. Yue-Jian, C.; juan, T.; Fei, X.; Jia-Bi, Z.; Ning, G.; Yi-Hua, Z.; Ye, D.; Liang, G. D. *Dev. Indust. Pharm.* **2010**, *36*, 1235.
11. Laurent, S.; Forge, D.; Port, M.; Roch, A.; Robic, C.; Elst, L. V.; Muller, R. N. *Chem. Rev.* **2008**, *108*, 2064.
12. Mok, H.; Zhang, M. *Exp. Opin. Drug. Del.* **2013**, *10*, 73.
13. Gonzllez-Tello, P.; Camacho, F.; Bllzquez, G. *J. Chem. Eng. Data*. **1994**, *39*, 611.
14. Zhang, Y.; Kohler, N.; Zhang, M. *Biomaterials*. **2002**, *23*, 1553.
15. Weissleder, R.; Bogdanov, A.; Neuweltb, E. A.; Papisov, M. *Adv. Drug. Del. Rev.* **1995**, *16*, 321.
16. Edwards, D. A., Deaver, D. R.; Langer, R. S. U.S. Pat. US5985320 A (**1999**).
17. Abbasi, N. N. M.Sc. Thesis, University of Guelph, **2013**.
18. Bridot, J. -L.; Stanicki, D.; Laurent, S.;. S.; Boutry, Y.; Gossuin, P.; Leclère, R.; Lazzaroni, L.; Vander Elst, R.; Muller, N. *Cont. Med. Mol. Imag.* **2013**, *8*(8), 466.
19. Javanbakht, T.; Laurent, S.; Stanicki, D.; Wilkinson, K. J. *PLoS One*. **2016**, *11*, e0154445.
20. Javanbakht, T.; Laurent, S.; Stanicki, D.; Raphael, W.; Tavares, J. R. *J. Nanopart. Res.* **2015**, *17*, 462.
21. Javanbakht, T.; Bérard, A.; Tavares, J. R. *Can. J. Chem.* **2016**, *94*, 744.
22. Couderc, H.; David, E. *Trans. Electr. Electron. Mater.* **2014**, *15*, 291.
23. León, A.; Reuquen, P.; Garin, C.; Segura, R.; Vargas, P.; Zapata, P.; Orihuela, P. A. *Appl. Sci.* **2017**, *7*, 49.
24. Polu, A. R.; Kumar, R. E. *J. Chem*. **2011**, *8*, 347.
25. Klonos, P.; Kaprinis, S.; Zarko, V. I.; Peoglos, V.; Pakhlov, E. M.; Pissis, P.; Gun'ko, V. M. *J. Appl. Polym. Sci*. **2013**, *37956*, 1601.
26. Jonscher, A. K. In Universal relaxation law; Chelsea Dielectric Press: London, **1996**.